Supporting Informations

Conversion of sewage sludge into high-performance bifunctional electrode materials for microbial energy harvesting†

Yong Yuan,[a] Ting Liu,[a,b] Peng Fu,[a,c] Jiahuan Tang,[a] and Shungui Zhou*[a]

[a] Guangdong Key Laboratory of Agricultural Environment Pollution Integrated Control, Guangdong Institute of Eco-Environmental and Soil Sciences, Guangzhou 510650, China

[b] Orient Science & Technology College, Hunan Agricultural University, Changsha 410128, China

[c] School of Chemical Engineering and Light Industry, Guangdong University of Technology, Guangzhou 510006, China

*Corresponding Author:

Phone: 86-20-3730-0951; Fax: +86-20-8702-5872;

email: sgzhou@soil.gd.cn

Table S1

Table S1. Element contents and electrochemical performance of electrodes

Anodes	C%	O%	N%	Fe%	P%	BET (m^2/g)	Biomass (μg protein cm^{-2})	EIS (Ω)		Power density (mW m^{-2})
								R_s	R_{ct}	
SM-0	9.4	48.1	1.27	4.8	5.43	16 ± 3	871 ± 25	36 ± 4	27 ± 3	486 ± 18
SM-5	37.5	36.8	1.16	3.4	3.15	24 ± 5	911± 30	27 ± 2	9 ± 2	787 ± 17
SM-10	46.1	32.5	1.09	2.7	2.55	36 ± 2	1191± 20	23 ± 2	4 ± 1.5	1069 ± 15
SM-20	59.2	26.9	0.92	2.2	1.63	54 ± 5	1131± 24	20 ± 2	2 ± 1	927 ± 16
GP	96.2	2.8	/	/	/	5 ± 1	881± 18	20 ± 2	39 ± 4	410 ± 10
CP	82.9	11.1	0.59	/	0.28	92 ± 8	956± 16	21 ± 1	12 ± 2	788 ± 39

/ undetactable; the power densities were achieved from the MFCs with the Pt/C cathodes; Error bars represent ± SD (n= 3)

Figure S1

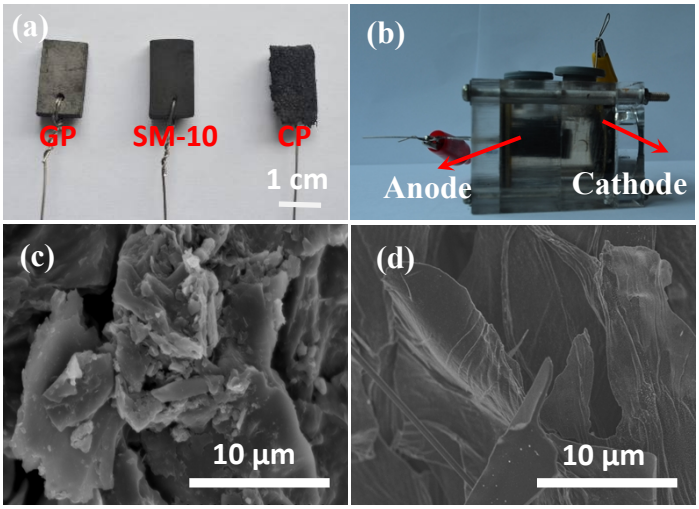

Figure S1. (a) Photographic illumination of the as-prepared anodes; (b) photographic image of the MFC equipped with the as-prepared anodes; (c) SEM image of the graphite plate (GP) anode; (d) SEM image of the coconut shell-derived carbon plate (CP) anode.

Figure S2

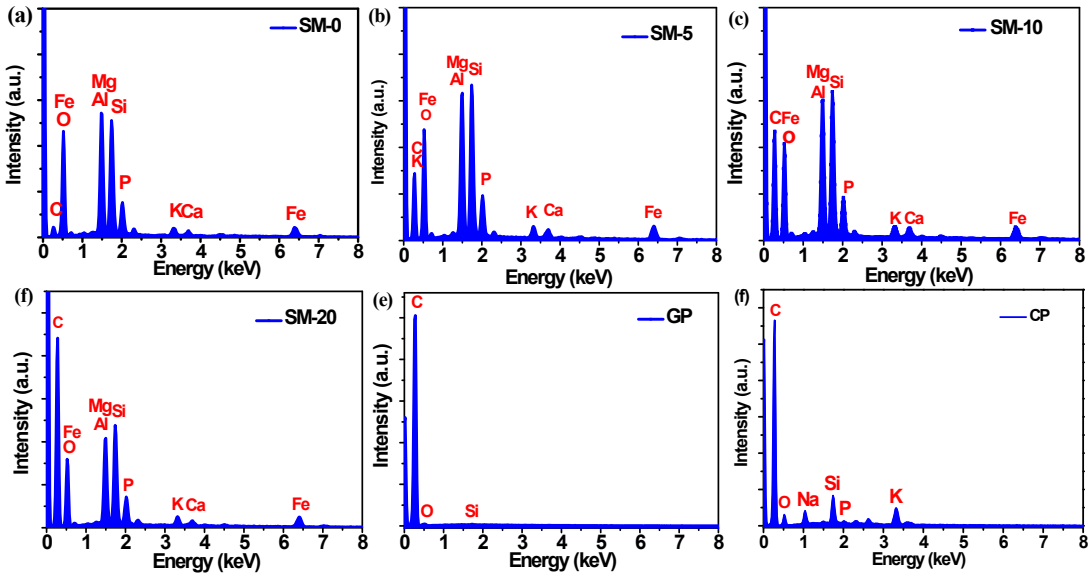

Figure S2. EDX spectrum showing the elemental composition of the resultant anodes.

Figure S3

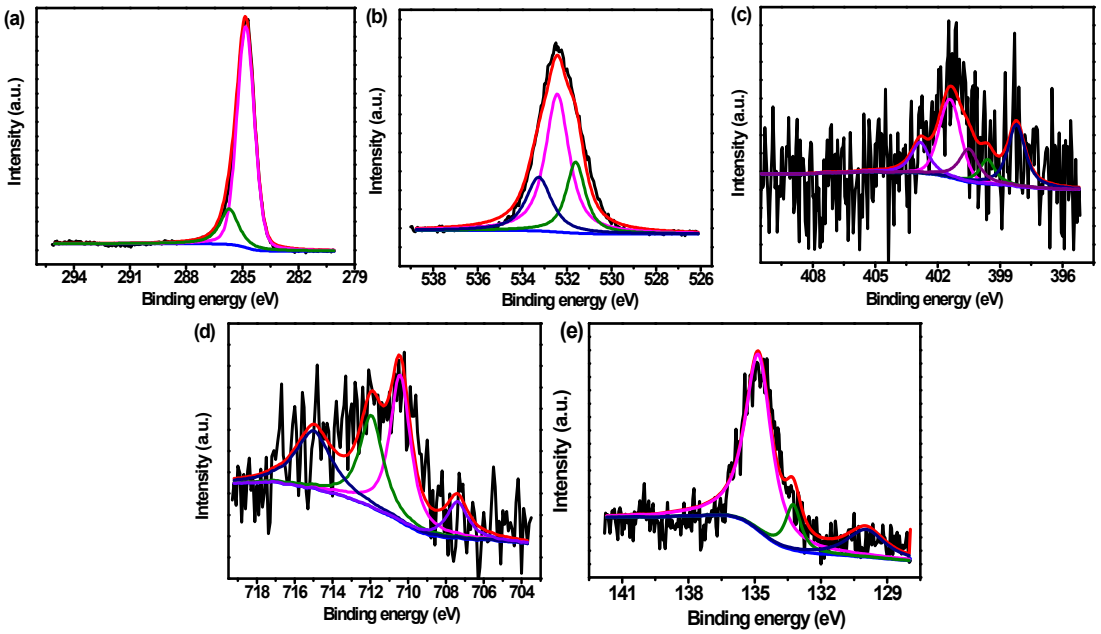

Figure S3. C1s (a), O1s (b), N1s (c), Fe2p (d) and P2p (e) core-level XPS spectra of SM-10.

Figure S4

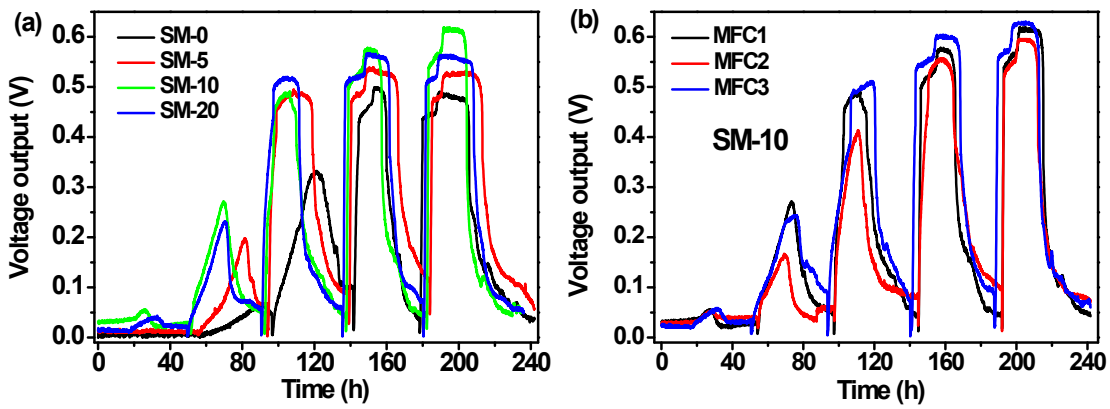

Figure S4. (a) Voltage output versus time curves during start-up of the MFCs with various anodes with a 1 kΩ reasistance loading; (b) Voltage output versus time curves of three parallel MFCs with the SM-10 anode.

Figure S5

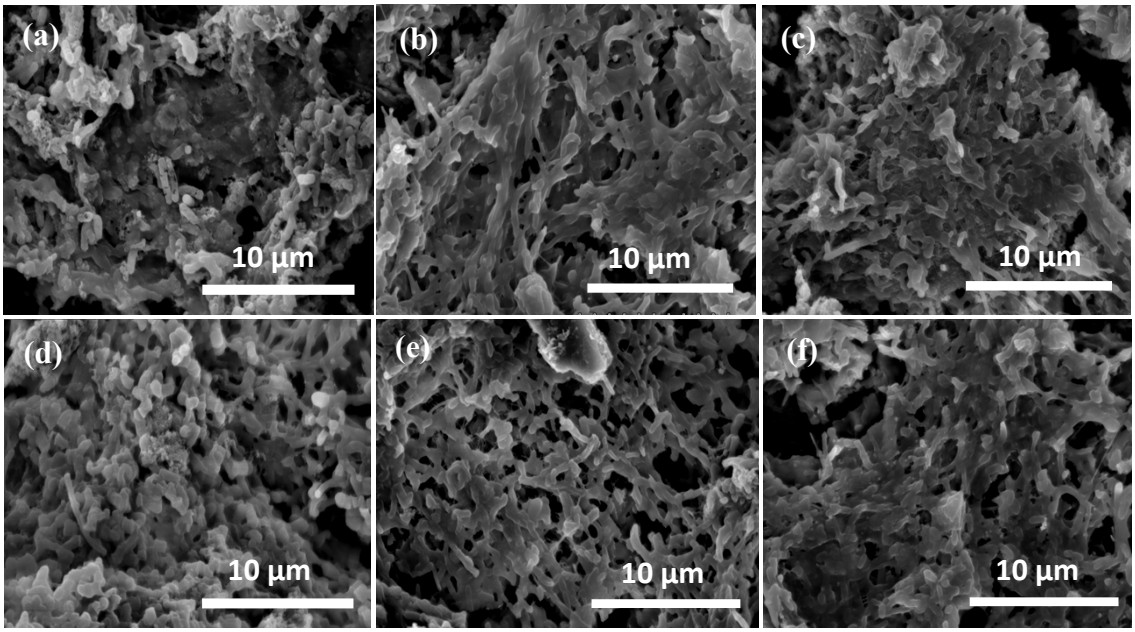

Figure S5. SEM images of the electroactive biofilm grown on the (a) SM-0, (b) SM-5, (c) SM-10, (d) SM-20, (e) GP and (f) CP andoes.

Figure S6

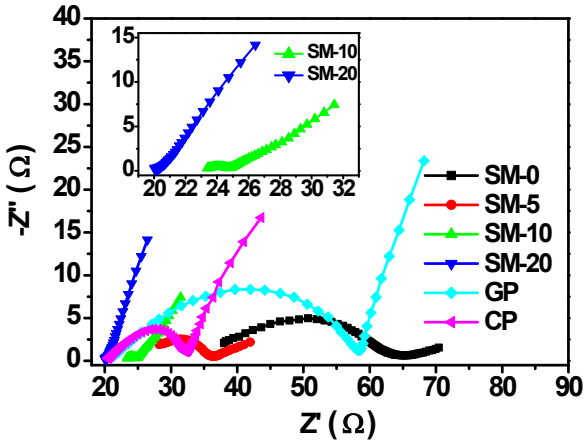

Figure S6. (a) Nyquist plots of the different anodes in the MFCs after inoculation. The inset contains Nyquist plots of the SM-10 and SM-20 anodes.

Figure S7

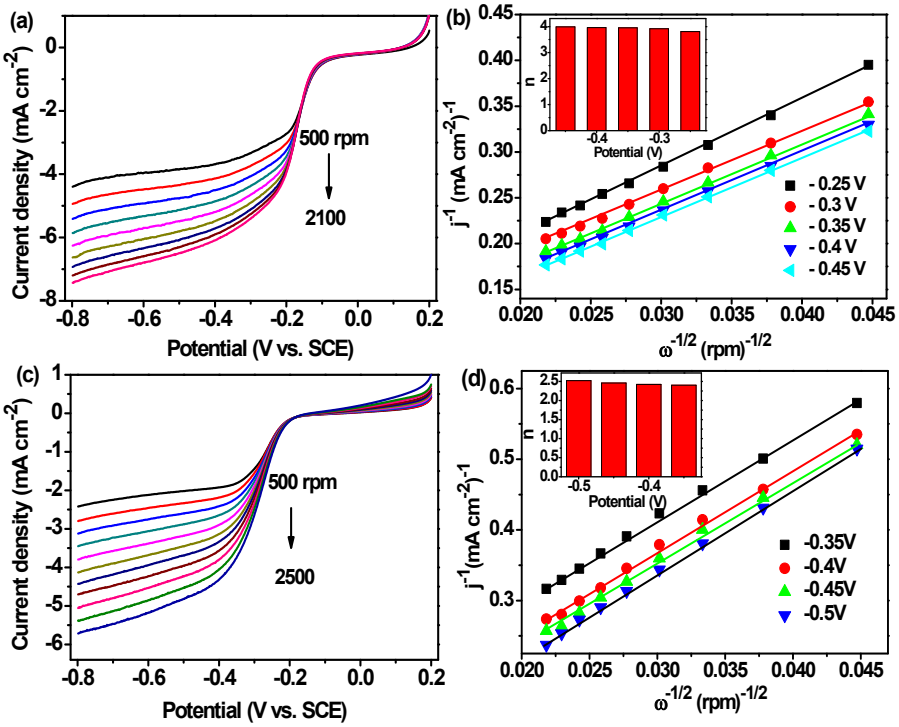

Figure S7. (a) RDE voltammograms of the Pt/C in O_2-saturated 0.1 M KOH collected with a sweep rate of 10 mV/s at various rotation speeds; (d) corresponding Koutecky-Levich plots (j^{-1} *vs.* $\omega^{-0.5}$) at different potentials on the Pt/C electrode (Inset: the estimated electron-transfer numbers at various potentials); (c) RDE voltammograms of the PSM-0 in O_2-saturated 0.1 M KOH collected with a sweep rate of 10 mV/s at various rotation speeds; (d) corresponding Koutecky-Levich plots (j^{-1} *vs.* $\omega^{-0.5}$) at different potentials on the PSM-0 electrode (Inset: the estimated electron-transfer numbers at various potentials)

In the Koutecky-Levich (K-L) plots of the catalysts, the relationship between 1/j and ω-1/2 was linear in the related potential regions. The K-L equations (eqs. 1 and 2) were used to further explore the reaction performance:

$$1/j=1/j_k+1/B\omega^{1/2} \qquad (1)$$

$$B=0.2nFC(D)^{2/3}\nu^{-1/6} \qquad (2)$$

where j is the measured current density, j_k is the kinetic limiting current density, B is the Levich slope, ω is the rotation speed, n is the total number of electrons transferred during ORR, F is the Faraday constant, C is the bulk O_2 concentration in the electrolyte, D is the O_2 diffusion coefficient, and ν is the kinematic viscosity of the electrolyte. The number of electrons transferred during the ORR process was determined using Eqs. (1) and (2).

Figure S8

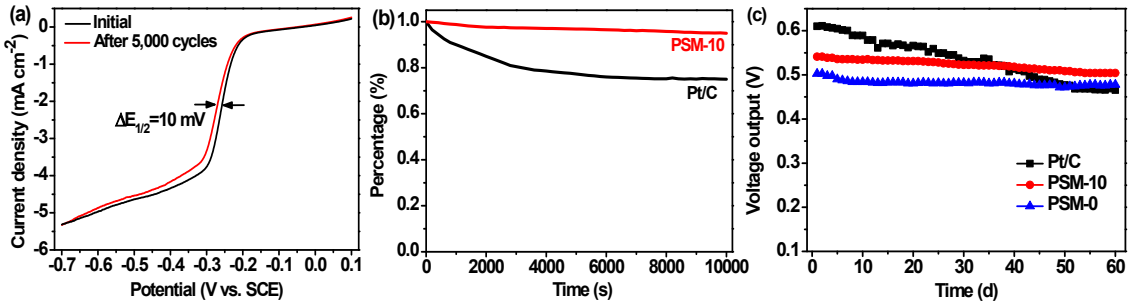

Figure S8. (a) RDE polarization curve of PMS-10 with scan rate of 10 mV/s before and after 5000 scanning cycles in O_2-saturated 0.1 M KOH; (b) Chronoamperometric responses (percentage of current retained versus operation time) of the kept at −0.40 V versus SCE in O_2-saturated 0.1 M KOH electrolyte at a rotating rate of 1100 rpm; (c) long-term stability tests of the MFCs with the SM-10 anodes and different cathodes (the voltage outputs were examined at 1000 Ω).